

# Magnetic Fields and Induced Voltages inside LPZ 1

## Measured at a 1:6 Scale Model Building

W. Zischank<sup>1</sup>, F. Heidler<sup>1</sup>, J. Wiesinger<sup>1</sup>, K. Stimper<sup>1</sup>, A. Kern<sup>2</sup>, E. Seevers<sup>3</sup>

1: University of the Federal Armed Forces Munich, Werner-Heisenberg-Weg 39, 85579 Neubiberg, Germany

2: Aachen University of Applied Sciences, Ginsterweg 1, 52428 Juelich, Germany

3: Hamburgische Electricitätswerke AG, Überseering 12, 22297 Hamburg, Germany

**Abstract:** For the application of the concept of Lightning Protection Zones (LPZ), the knowledge of the magnetic fields and induced voltages inside a structure is necessary. Laboratory experiments have been conducted at a down-scaled model of a building (scale factor 1:6) to determine these electromagnetic quantities in case of a direct strike to the structure. The model (3 m x 2 m x 2 m) represented a small industrial building using the reinforcement of the concrete as electromagnetic shield. The magnetic fields and magnetic field derivatives were measured at several location inside the scaled model. Further, the voltages induced on three typical cable routes inside the model was determined. The influence of the lightning current wave-shape, point-of-strike, bonding of the cable routes, and bridging of an expansion joint in the middle of the building on these quantities was studied.

**Keywords:** Lightning, electromagnetic shielding, reinforced concrete, scaled model.

### 1. Introduction

Direct lightning strikes constitute a severe threat to sensitive electrical or electronic equipment located inside a structure. Due to the ever increasing use and sensitivity of micro-electronic circuits and due to the interconnection of equipment by extended information technology networks during the last few decades, the control of the electromagnetic interferences has become the dominant task of lightning protection. As the basic philosophy to control lightning generated electromagnetic interferences, the principle of "Lightning Protection Zones (LPZ)" has been developed by the committee IEC TC 81 and has been laid down in the international standard series IEC 62305 [1,2]. The principle of LPZs requires to form nested zones of successively reduced electromagnetic environment. This objective is achieved by a) shielding to reduce the electromagnetic fields and b) equipotential bonding of all lines at the LPZ-boundaries to limit the line conducted overvoltages and currents.

A cost effective method to form electromagnetic shields is to use existing metallic structural components, like the reinforcement of concrete. Such structural shields, of course, are leaky shields and therefore it is necessary to know about their effectiveness in reducing the electromagnetic environment. Theoretical computation of magnetic fields inside steel structures formed by grid-like spatial shields has been presented in [3, 4]. Few experimental work has been done, e.g. [5].

In IEC 62305-4 [2] equations for the assessment of the magnetic fields and induced voltages inside grid-like spatial shields caused by a direct strike to the structure are given as a function of mesh width and location inside the structure. These equations do not exactly represent the field inside for a given configuration. Moreover, they are worst case curves derived from the computation [3, 4] of numerous configurations of buildings or structures consisting of a single-layer metallic grid-like shield. These numerical simulation, however, were limited to a minimum mesh width of about 40 cm and had to be extrapolated for smaller mesh width (typical 15 cm for practical reinforcement of concrete). Furthermore the resistances of the current-carrying reinforcement rods and capacitive coupling were neglected. Therefore, frequency dependent effects as well as transient phenomena were disregarded for the IEC-formulae. In a previous paper [6] the additional shielding effectiveness of a second layer of reinforcement grid had been analysed. Object of this study was to experimentally validate the assessment formulae of IEC 62305-4. In this paper only the experimental results will be presented. The comparison of experimental results to the IEC assessment formulae will be discussed in an accompanying paper [7].

### 2. Scale Factors

In order to determine the electromagnetic environment inside an LPZ 1, scale modeled structures have been set

up in the High Current Laboratory of the University of the Federal Armed Forces in Munich (UAFM).

Measurements at scaled models necessitate that not only the geometry, but all relevant physical quantities have to be scaled according to the laws of the similarity theory. A detail description of the derivation of scale laws is given in [8]. Under the prerequisite that the permeability  $\mu$  and the dielectric constant  $\epsilon$  of the model and the real structure be the same, the scale factors relevant to the experiments conducted can be derived (Table 1). The relationship between a physical quantity of the model  $Q_m$  and the same quantity of a real structure  $Q_r$  is given by

$$Q_m = Q_r / M, \text{ with } M \text{ being the scale factor.}$$

Quantity	Length	Time	Current	Conductivity
Unit	m	s	A	S/m
Factor	M	M	M	1/M

**Table 1: Scale factors**

The scale factor was chosen to  $M = 6$ , mainly because of material considerations: The ratio of the conductivity of steel (real reinforcement) to that of copper (model structure) is about 1:6. Due to the laboratory size, the scaled model dimensions were limited to 3 m x 2 m x 2 m. With the scale factor  $M = 6$  this represents a small industrial building with a base of 18 m x 12 m and a height of 12 m.

### 3. Test Setup

The experiments comprised four models, labeled BI through BIV. In the following only the dimensions of the down-scaled model will be given. The dimension of a corresponding real-size building can be determined by multiplication with the scale factor  $M = 6$ .

#### 3.1 Reference Model BI

Model BI simulated a structure with a “classical” external lightning protection system according to lightning protection level I of IEC 62305-3 [9]. Model BI was intended as a reference by which the improved shielding of grid-like structures could be judged. The air termination was formed by a meshed wire system of 0,66 m x 1,5 m. The model BI had 6 down conductors, 4 at the edges and 2 in the middle of the long sides. For the air termination and the down conductors copper wires with a diameter of 2 mm were used. The wires were soldered at all intersections. The base of the model consisted of a 2 mm copper plate simulating ideal ground. The down conductors were soldered to this ground plate.

#### 3.2 Model BII

Model BII represented a building with an ideally interconnected grid-like shield of two layers of reinforced concrete. It is well known that the concrete itself does not significantly contribute to the electromagnetic shielding. Therefore, the scale modeled structure simulated only the double-layer steel reinforcement of the concrete. The

reinforcement of the roof and the side walls was simulated by copper grids having a mesh width of 20 mm. The wire diameter of the grids was 1,5 mm. The distance of between the two grid layers was 25 mm. At the edges of the grids all individual wires were soldered. Also all wires of the grids were soldered to the 2 mm copper ground plate. The inner and outer reinforcement layers were connected by 1,5 mm copper wires in a 200 mm spacing.

#### 3.3 Model BIII

Model BIII had the same basic construction as model BII. It was used to study the influence of a) additional connections between the cable trays and the inner reinforcement and b) the interconnection of the individual segments of the cable trays.

#### 3.4 Model BIV

Model BIV was intended to study the effects of the bridging of an expansion joint in the middle of a building. To this end, model BII was cut in the center in two halves and the resulting expansion joint was bridged by 2 mm copper wires at the inner reinforcement layer. The number of bridge wires was varied from 2 up to 24.

## 4. Magnetic Field Measurement

The magnetic fields and their derivatives were determined at four locations inside the models (figure 1). The first location was in the center of the models. The other 3 locations were at half-height of the models (i.e. 1 m above the ground plate) in a distance of 0,75 m to the smaller (right) side wall. The distances to the long side wall were 5,5 cm, 0,5 m und 1 m, respectively.

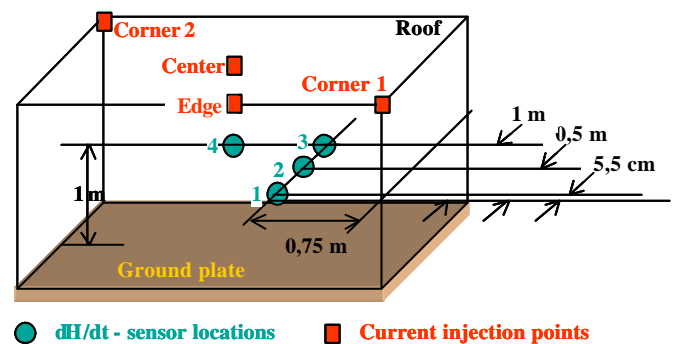


**Figure 1: Sensors location and current injection points**

The x, y and z components (definition of coordinates see figure 2) of the magnetic field derivatives ( $dH/dt$ ) were measured using shielded loop sensors of 6 cm, 15 cm and 20 cm diameter. The corresponding bandwidth of the sensors were 70 MHz, 22 MHz and 16 MHz, respectively. The signals were transferred to the digital scopes (HP 54510A, 200 MHz single shot bandwidth) via 300 MHz fiber optic link systems NanoFast OP 300-2A. The magnetic fields were derived from the ( $dH/dt$ )-waveforms by numeric integration. Background noise originating from the current generator spark gaps (start gaps, crowbar gap,

peaking circuit gaps) was eliminated during the integration process.

### 5. Cable Trays

Model BII was equipped with the simulation of 3 typical cable trays. Figure 2 shows the arrangement of the cable trays inside the model.

Cable tray 1 (CT1) started 25 cm below the roof, leading 50 cm along the roof towards the edge, then, in a distance of 25 cm to the side walls, down to a level 25 cm above the ground plate and at this level all along the long side of the model towards the opposite side wall.

Cable tray 2 (CT2) started in a distance 25 cm to the side walls, leading at a level of 25 cm below the roof all along the long side of the model, then down to a level of 25 cm above the ground plate and from there to the side wall.

Cable tray 3 (CT3) was running vertically from the roof to the ground plate along the edge of the model with a distance of 25 cm to the adjacent side walls.

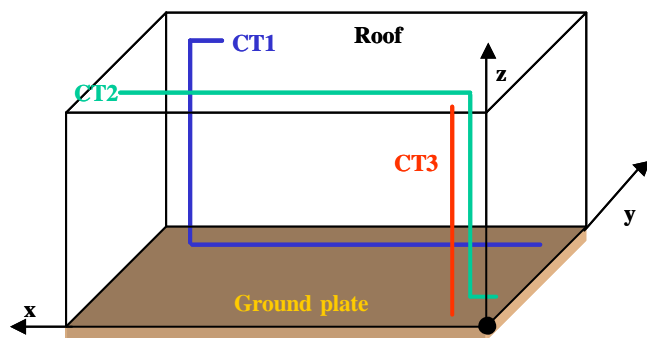


Figure 2: Routing of cable trays

Figure 3 shows a section of the scaled cable trays consisting of 50 cm long sections made of 1 mm sheet copper. The individual sections were interconnected by 1 mm copper wires. At both ends, the cable trays were connected by 1 mm copper wires to the inner reinforcement layer / ground plate the shortest possible way.

A 2 mm sensor wire was located in the middle of each cable tray. At the roof side the wire was connected to the cable tray's metal structure. At the bottom side the sensor wire terminated into a fiber optical transmission system (50 Ω input) to measure the induced voltage along the cable tray.

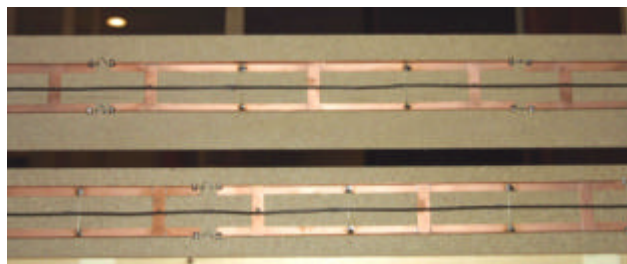


Figure 3: Section of the scaled cable trays

### 6. Test Currents and Generators

It was intended to simulate two impulse current waveforms:

- a positive stroke current of 200 kA, 10/350 μs according to IEC 62305-1 [1];
- a negative first stroke current of 100 kA, 1/200 μs according to the German standard KTA 2206 [10] for the lightning protection of nuclear power plants.

Table 2 gives the main parameters (current peak value  $i_{max}$ , front time  $T_1$  and decay to half value  $T_2$ ) of the test currents as defined in the standards, the down-scaled parameters for  $M = 6$  and the parameters actually obtained in the model experiments. It was not possible to simulate the waveform 0,25/100 μs [1] of negative subsequent strokes: The down scaled front time of 0,25 μs/6 ≈ 40 ns could not be implemented in the laboratory at the models with physical dimension of several meters.

		$i_{max}$ (kA)	$T_1$ (μs)	$T_2$ (μs)
Positive stroke	IEC 62305	200	10	350
	Scaled M=6	33,3	1,67	58,3
	Experiment	18	1,8	57
Negative first stroke	KTA 2206	-100	1	200
	Scaled M=6	-16,7	0,167	33,3
	Experiment	-5,5	0,25	12

Table 2: Test current parameters of model B

Primary objective for the design of the impulse current generators was to achieve the required front time as close as possible. The positive stroke currents were generated by an over-critically damped 100 kJ capacitor bank with an additional peaking capacitor. The negative first stroke currents were obtained from a 250 kV three-stage Marx generator with an erected capacitance of 400 nF equipped with a low impedance peaking capacitor and a peaking spark gap.

The currents were injected at 4 locations of the roof: to the center, to the edge of one long side and to two opposite corners as indicated in figure 5.

The models were placed on a wooden support rig, 1,5 m above laboratory floor. In order to facilitate a symmetric arrangement of the models with respect to the test current generator, the models had to be rotated by 90° (i.e. the roof is pointing to the left and the floor to the right). Figures 4 and 5 illustrate the arrangement of the test structure on the test rig. The current return paths from the ground plate was formed by an array of eight copper return conductors (10 mm<sup>2</sup> each) that were quasi-coaxially arranged around the models in a distance of 1 m to the side walls.

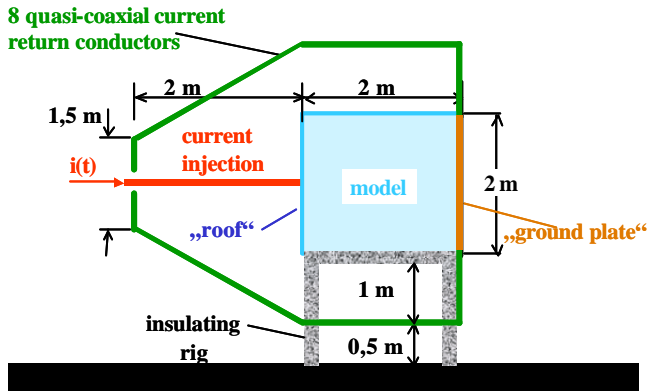


Figure 4: Schematic representation of the test setup

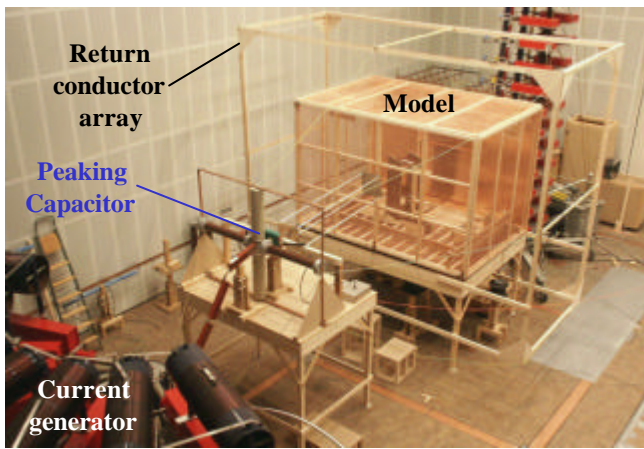


Figure 5: Test setup in the laboratory

## 7. Resulting Waveshapes

For the classical external lightning protection system model BI, the measured waveshapes of the magnetic field and the magnetic field derivative were in good agreement to waveshapes of the injected current and current derivative, as shown in Figure 6 for the normalized magnetic field  $H^*$  and current  $i^*$ . As an example, Figure 6 shows the x-component of the sensor located in the center of the model for a positive stroke injected to the edge of the roof.

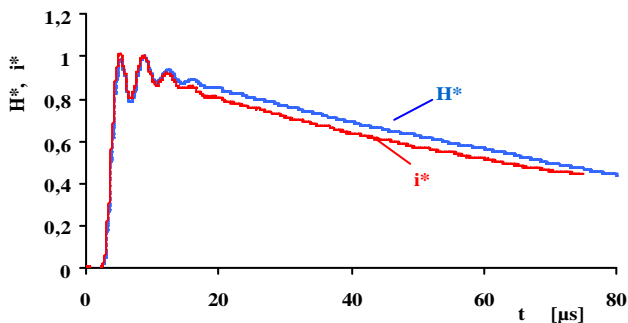


Figure 6: Normalized magnetic field  $H^*$  and injected current  $i^*$  for model BI

For the model BII with the grid-like reinforcement shield the waveshapes of current and magnetic field were substantially different. As an example, Figures 7 and 8 show the x-component of the sensor located 50 cm from the side wall of the model for a positive stroke injected to the center of the roof. The zero crossing of the  $dH/dt$  (Figure 7) does not occur around the current peak value, but clearly later, when the current has almost ceased. As a consequence, the magnetic field rise is much slower compared to the injected current rise (Figure 8). This effect has also been observed in [6].

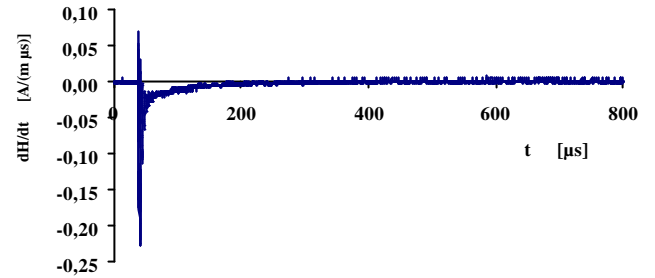


Figure 7: Magnetic field derivative for model BII

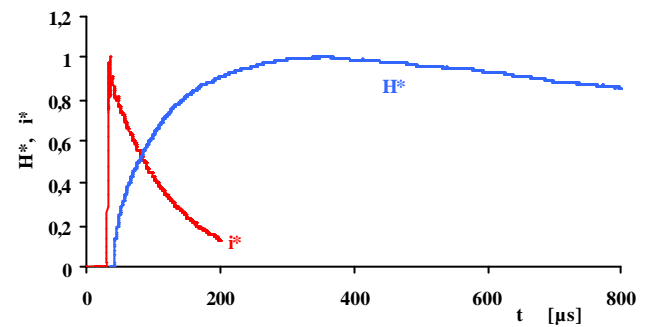


Figure 8: Normalized magnetic field  $H^*$  and injected current  $i^*$  for model BII

An example of the voltage induced to the sensor wire on the cable tray is given in Figure 9 for CT1 and injection of a positive stroke to the roof center. The current along the cable tray has, similar to the magnetic field  $H$  in Figure 8, a substantial slower rise compared to the injected current.

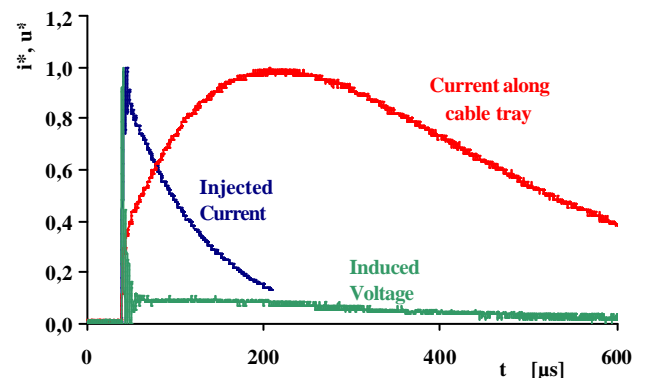


Figure 9: Normalized injected current, current along the cable tray and induced voltage

The induced voltage starts with a sharp peak which is about proportional to the steepness  $di/dt$  of the injected current. The sharp peak is followed by a slow decay, which is mainly due to the resistive voltage drop along the cable tray. At the instant of the peak of the current along the cable tray, where  $di/dt$  is zero, the voltage corresponds well to the d.c. resistance of the cable tray multiplied by the current.

### 8. Measurement results and discussion

The peak values of the measured magnetic field derivatives  $dH/dt$  and the resulting magnetic fields  $H$  for model BII are given in Table 3 (positive stroke) and in Table 4 (negative first stroke) for the different current injection points. The sensor locations 1 ... 4 can be seen from Figure 1. A comparison of these experimental results to that of the formulae given in IEC 62305-4 [2] will be given in an accompanying paper [7].

Injection	dH/dt [A/(m·μs)]				H [A/m]			
	1	2	3	4	1	2	3	4
center	0,27	0,31	0,18	0,17	2,21	2,56	3,86	1,84
edge	0,76	0,96	1,10	1,09	8,27	12,3	10,6	12,6
corner 1	0,63	1,03	1,06	0,64	7,69	12,5	13,5	8,98
corner2	0,29	0,42	0,00	0,41	3,61	5,22	0,00	5,18

Table 3: Results for model BII, positive stroke

Sensor	dH/dt [A/(m·μs)]				H [A/m]			
	1	2	3	4	1	2	3	4
center	1,27	1,29	2,29	1,12	0,25	0,16	0,24	0,23
edge	2,17	2,66	4,27	2,46	0,56	0,51	0,67	0,62
corner 1	3,19	1,48	4,17	2,14	0,66	0,17	0,69	0,09
corner2	1,66	1,06	1,67	1,89	0,29	0,12	0,17	0,29

Table 4: Results for model BII, negative first stroke

In order to characterize the effect of a grid-like shield, the peak values of  $H$  and  $dH/dt$  for the models BI and BII are compared. Table 5 gives the ratios  $H_{BI}/H_{BII}$  and  $dH_{BI}/dH_{BII}$  for both stroke types as factors and in decibel.

There is a wide scatter of the ratios between the minimum and maximum values. The reduction of the electromagnetic field depends much on the current injection point and the sensor location inside the models. Except for the magnetic field of the positive stroke, however, a reduction of at least 40 dB can be achieved, when using a double layer steel reinforcement as grid-like shield.

Stroke		Ratio $H_{BI} / H_{BII}$		
		Mean	Max	Min
Positive	BI / BII	105	667	17
	dB	40	56	24
Negative first stroke	BI / BII	596	2000	84
	dB	55	66	39
		Ratio $dH_{BI} / dH_{BII}$		
		Mean	Max	Min
Positive stroke	BI / BII	796	2950	108
	dB	58	69	40
Negative first stroke	BI / BII	734	2920	135
	dB	57	69	43

Table 5: Ratios for H and dH/dt

### 9. Bonding of cable trays

With the experiments at model BIII variations of the bonding of the cable trays were studied. In a test series BIIIa additional connections between the cable trays and the inner reinforcement were installed every meter. To characterize the effect of additional bonding, the ratios of the peak values of the induced voltage measured at model BII and BIIIa are presented in Figure 10. All ratios BII / BIIIa are about 1. The additional bonding to the inner reinforcement therefore has no noticeable effect!

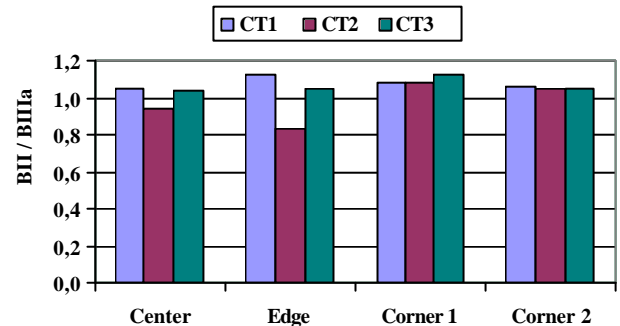


Figure 10: Effect of additional bonding to the inner reinforcement

In a test series BIIIb all the interconnection of the individual segments of the cable trays were removed. To characterize the effect of interconnecting the segments, the ratios of the peak values of the induced voltage measured at model BIIIb and BII are presented in Figure 11. The mean value of the ratios BIIIb / BII is 5,7 with a standard deviation of 0,56. Interconnecting the cable tray segments thus reduces the induced voltages by a factor of nearly 6.

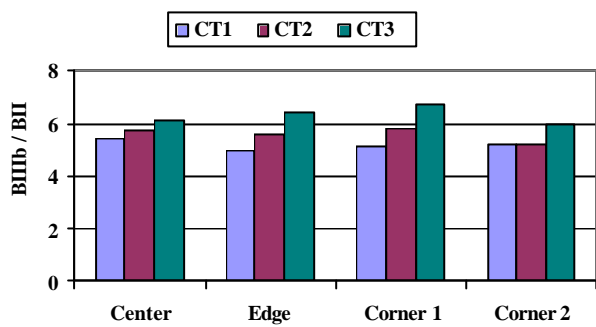


Figure 11: Effect of bonding of the cable tray segments

### 10. Influence of expansion joints

Large reinforced concrete walls usually have to be interrupted by expansion joints. Such expansion joints constitute a discontinuity of the electromagnetic shield and have to be bridged, e.g. by copper braid bonds. To study the influence of expansion joints and their bridging a test series BIV was conducted. Model BII was cut in the center in two halves and the resulting expansion joint was bridged by 2 mm copper wires at the inner reinforcement layer. The number of bridge wires was varied from 2 up to 24.

To characterize the effect of the bridging of an expansion joint, the ratios of the peak values of the cable tray induced voltages are compared for model BIV and BII. Figure 12 shows the ratios BIV / BII as a function of the number of bridging wires for the 3 cable trays. using only few bridging wires (2 or 4) results in an increase of the induced voltage by a factor of 100 to more than 1000. Only for cable tray CT3 the effect is not so pronounced: CT3 is the vertical cable tray located along the edge of the model and does not lead across the expansion joint. A large number of bridging connections is required in order to keep the increase of the induced voltage below a factor of 10. For a real size building this means a distance of not more than 1 m ... 2 m between the bridging connections.

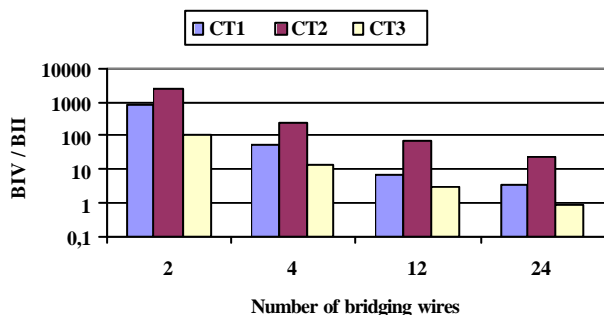


Figure 12: Effect of the bridging of an expansion joint

### 5. Conclusion

Laboratory experiments have been conducted at a down-scaled model of a building (scale factor 1:6) to determine the electromagnetic quantities in case of a direct strike to the structure. It is found that the use of the double layer reinforcement steel as a grid-like shield reduces the magnetic field change  $dH/dt$ , which is responsible for induced voltages, by at least 40 dB. It was found that additional bonding of cable trays to the inner reinforcement layer has no noticeable effect. In order to keep induced voltage low, a good lengthwise bonding of cable trays is necessary and expansion joints in the wall of a building have to be bridged at least every 1 m ... 2 m.

### 7. References

- [1] IEC 81/216/CDV / IEC 62305-1, Ed. 1:2003-05: "Protection against lightning – Part 1: General Principles".
- [2] IEC 81/238/CDV / IEC 62305-4, Ed. 1:2003-12: "Protection against lightning – Part 4: Electrical and electronic systems within structures".
- [3] König M.: "Transient overvoltages in large buildings with natural components during a direct strike", 23rd Int. Conf. on Lightning Protection (ICLP), Firenze (I), 1996, pp. 545-550.
- [4] König M., Steinbigler H.: "Magnetic field distribution inside a gridlike spatial shield in case of a direct lightning strike", 24th Int. Conf. on Lightning Protection (ICLP), Birmingham (UK), 1998, pp. 264-269.
- [5] Schnetzer G.H., Fisher, R.J.: "Measured responses of a munitions storage bunker to rocket-triggered lightning", 21st Int. Conf. on Lightning Protection (ICLP), Berlin, Germany, 1992, pp. 237-242.
- [6] Zischank W., Heidler F., Wiesinger J., Kern A., Seevers M., Metwally I.: "Laboratory simulation of direct lightning strokes to a modelled building - measurement of magnetic fields and induced voltages", 26th Int. Conf. on Lightning Protection ICLP 2002, Cracow, Poland, September 2002, paper 7b.4, Conference Proceedings Volume II, pp. 591-596.
- [7] Kern A., Zischank W., Heidler F., Seevers M.: "Magnetic fields and induced voltages in case of a direct strike – comparison of results obtained from measurements at a scaled building to those of IEC 62305-4", 27th International Conference on Lightning Protection (ICLP), Avignon (F), 2004.
- [8] Frentzel, R.: "Use of similarity relations in the analysis of lightning-induced transient phenomena", European Transactions on Electrical Power, ETEP, Vol. 7, No. 3, May/June 1997.
- [9] IEC 81/240/CDV, IEC 62305-3, Ed. 1: 2004-01: "Protection against lightning - Part 3: Physical damage to structures and life hazard".
- [10] KTA 2206: 2000-06: „Auslegung von Kernkraftwerken gegen Blitzeinwirkungen“. Safety guidelines of KTA.